Theor Chem Acc (2013) 132:1312
DOI 10.1007/s00214-012-1312-x

REGULAR ARTICLE

Low-energy nanoscale clusters of $(TiC)_n$ $n = 6, 12$: a structural and energetic comparison with MgO

Oriol Lamiel-Garcia · Stefan T. Bromley · Francesc Illas

Received: 31 October 2012 / Accepted: 28 November 2012 / Published online: 22 January 2013

Abstract Global optimization and density functional theory-based calculations are used to investigate the structure of $(TiC)_6$ and $(TiC)_{12}$ clusters. In both cases, the isomers exhibiting the bulk-like rock salt structure appear to be the most energetically stable. This is in contrast to a number of other materials that have the rock salt structure as their bulk ground state, such as MgO, for which more open tubular motifs are observed. A major factor contributing to this difference in nanoscale structure is likely to be the larger covalent character of TiC as compared to MgO. This is supported by our finding that some of the low-energy isomers of both $(TiC)_6$ and $(TiC)_{12}$ exhibit C–C bonding, whereas the bonding in all analogously sized MgO isomers is solely based on Mg–O ionic bonding. The simulated IR spectra indicate that it should be experimentally possible to differentiate $(TiC)_n$ clusters with or without C–C bonds.

Published as part of the special collection of articles derived from the 8th Congress on Electronic Structure: Principles and Applications (ESPA 2012).

Electronic supplementary material The online version of this article (doi:10.1007/s00214-012-1312-x) contains supplementary material, which is available to authorized users.

O. Lamiel-Garcia · S. T. Bromley · F. Illas (✉)
Departament de Química Física and Institut de Química Teòrica i Computacional (IQTCUB), Universitat de Barcelona, 08028 Barcelona, Spain
e-mail: francesc.illas@ub.edu

S. T. Bromley (✉)
Institució Catalana de Recerca i Estudis Avançats (ICREA), 08010 Barcelona, Spain
e-mail: s.bromley@ub.edu

Keywords TiC · Clusters · Nanoclusters · Density functional theory · Global optimization

1 Introduction

The technological need to improve our understanding of important inorganic solids (e.g. ZnO, SiC, TiO_2) at the nanoscale has renewed the interest in the detailed modelling of the atomic and electronic structure of nanosized clusters of such materials. Nanoclusters of only a few tens of atoms are placed somewhere between molecules and bulk-like nanoparticles of hundreds of atoms. Not only are nanoclusters thus fundamentally interesting for studying how a material's properties scale with increasing size, but also with respect to their physical or chemical properties which may significantly differ from those exhibited by larger nanoparticles and extended solids. Probing and exploiting the specific nanoscale properties of inorganic solids have become major objectives in numerous different fields such as nanotechnology, catalysis, solar cells, electronic components, and material science [1–5]. In addition to their singular properties, the study of inorganic nanoclusters can give insights into growth and nucleation processes which lead to different observed crystal structures [6, 7] in a given material and/or even suggesting the possible existence of new cluster-based materials [8, 9]. In this sense, the ability to predict the most stable ground state structures of nanoclusters, assumed to be those most likely to be found in the experiment, becomes an urgent and important subject. Exhaustive exploration of the potential energy surface of even small-sized clusters is a formidable task due to the large number of possible stable structures which grows exponentially with the number of atoms in the cluster. For this reason, different specific global

optimization approaches have been developed to efficiently search the low-energy isomer spectrum of nanoclusters [10–12]. In this study, we employ global optimization at a classical level of theory followed by refinement using quantum mechanical-based methods to investigate the most stable isomers of nanoclusters of titanium carbide (TiC) with six and twelve formula units.

TiC is a material in the fringe zone between ionic and covalent, with bonding properties that go from metallic, covalent, to ionic [6, 7]. Bulk TiC exhibits the rock salt structure which is commonly found in strongly ionic materials such NaCl or MgO, the latter being a prototypical non-reducible ionic oxide. In spite of its rather simple crystal structure, TiC has shown interesting properties, for instance in heterogeneous catalysis. In this context, TiC, and other simple transition metal carbides, has been suggested as the potential substitutes for expensive noble metal-based catalysts of the platinum group and, furthermore, can display advantages over these bulk transition metals in terms of catalytic selectivity or resistance to poisoning [13, 14]. Transition metal carbides have already proven to be efficient in some reactions of great technological importance, as the water–gas shift reaction [15], and received recent attention in a variety of processes [16–19]. In addition, transition metal carbides have proven to be an excellent support for metallic nanoparticles, especially after the pioneering work of Ono et al. [20] on the catalytic properties of Au nanoparticles supported on TiC. Subsequent work has shown that Au/TiC systems exhibit extraordinary reactivity in DeSOx reactions [21–23], being active to dissociate molecular oxygen [24] and molecular hydrogen [25, 26] and, more recently, even to hydrogenate CO_2 to methanol [27]. In the specific case of TiC, it has been shown that, for the water–gas shift reaction, small clusters adsorb reactants and products too strongly, thus resulting in excessively large energy barriers [15]. A deeper knowledge of TiC nanoparticles seems necessary to be able to properly tune their properties for such applications.

Non-stoichiometric clusters containing Ti and C are known since the early cluster beam work of Castleman and co-workers [28] who termed these clusters as metallocarbohedrenes, or just metcars, where Ti_8C_{12} was found to be particularly stable. These metcars have been studied in detail for a long time from both theoretical and experimental point of view [29–35]. Metcars were found to be especially stable and abundant when obtained by laser vaporization under certain experimental conditions and were clearly identified by mass spectroscopic techniques. Subsequent theoretical investigations were carried out to elucidate the geometry and structure of metcars, showing that they have a cage shape similar to fullerenes formed by pentagonal rings [28, 30]. These results increased the interest of the scientific community in the possible properties and utilities of these particular clusters [28–30]. Nevertheless, succeeding works found that, depending on the experimental conditions, metcars are not necessarily the most abundant and stable structures, with $Ti_{14}C_{13}$ and also larger 1:1 stoichiometric clusters, being found to be as abundant as the metcars or even more so [29, 30]. Such stoichiometric TiC clusters may also have relevance to astrophysical environments, with experimental measurements and observations both pointing to the presence of such clusters around stars as possible precursors in the nucleation of carbonaceous stardust [36].

In this work, we focus on the study of the ground state atomic structures of the stoichiometric $(TiC)_n$ clusters with $n = 6, 12$ and compare the lowest energy structures to the corresponding clusters exhibited by MgO. For the TiC clusters, we also calculate the vibrational IR spectra in order to find fingerprints to assist in the identification of such clusters in experiment.

2 Methodology and computational details

Since TiC and MgO exhibit the same bulk rock salt structure, it is interesting to see whether this correspondence also holds for the extreme case of small nanoscale clusters. For this comparison, we take the sizes $(TiC)_6$ and $(TiC)_{12}$ and use the structures of the low-energy isomers of the correspondingly sized MgO clusters obtained from global optimization calculations based on the basin-hopping algorithm [37] using simple ionic Born interatomic potentials. As nanocluster structures are highly dependent on the atomic charges employed in such potentials, in order to capture a wide structural variety, the effective ionic charges, $Mg^{q+}O^{q-}$, were varied (between 1e and 2e) and global optimizations were performed for each value of q [38, 39].

More than 15 different isomer structures resulting from the basin-hopping global optimizations were considered for $(TiC)_6$ and $(TiC)_{12}$ in a first round of calculations. The structures and energies of these isomers were first optimized employing a Lennard–Jones two body potential with an Axilrod–Teller potential for the three body interactions following the parameterization by Erkoc [40], using the General Utility Lattice Program (GULP) code [41]. The lowest energy geometries thus obtained were then refined using density functional theory (DFT)-based calculations performed with the VASP code [42–45]. In the DFT calculations, the valence electron density was expanded in a plane wave basis set with a cut-off of 415 eV for the kinetic energy and the effect of the core electrons on the valence density was taken into account using the projector augmented wave method [46, 47]. The exchange–correlation effects were described by the Perdew–Wang (PW91) [48, 49] implementation of the generalized gradient approach (GGA) functional. The calculations were

performed using a cubic cell of $20 \times 20 \times 20$ Å, to guarantee there was no significant interaction between the images of the replicated cells. All calculations were carried out considering the Γ point of the reciprocal space only. Structures were considered converged when forces on the atoms were smaller than 0.03 eV/Å.

In order to further confirm that the lowest energy optimized structures found in the PW91/DFT calculations corresponded to genuine energy minima on the potential energy surface, frequency calculations including dipole moment calculations were carried out. This type of calculation also allows one to compute the intensities corresponding to the lowest transition for each normal mode and thus simulate the infrared (IR) vibrational spectra. The dipole intensity of a given normal mode k corresponding to the z component (μ_z) of the dipole is computed according to the following expression [50–52]

$$I^k = \left(\frac{\partial \mu_z}{\partial Q_k}\right)^2 = \sum_{i=1}^{3n} \left(\frac{P_{ik}}{\sqrt{m_i}} \frac{\partial \mu_z}{\partial \Delta r_i}\right)$$

where μ_z is the z component of the dipole moment, Δr_i are the Cartesian displacements, and $\frac{P_{ik}}{\sqrt{m_i}}$ is the mass-weighted coordinate matrix of this normal mode. Summing the contributions for the x, y and z components permits one to obtain the full theoretical IR spectra for each of the considered structures of the $(TiC)_6$ and $(TiC)_{12}$ clusters.

3 Results and discussion

The ground state structures for both $(TiC)_6$ and $(TiC)_{12}$ are found to exhibit the bulk rock salt structure, see Fig. 1. In both cases, the $(TiC)_6$ and $(TiC)_{12}$ resemble small elongated rock salt slabs. The TiC distances in each of these clusters were found to be similar to the corresponding values in the bulk, but with a small contraction observed in the $(TiC)_6$ structure. This is most clearly noticeable for the TiC bonds at the ends of the cuboid $(TiC)_6$ cluster and can probably be attributed to the low coordination of these surface atoms together with the relatively small cluster size. In the case of $(TiC)_{12}$, the bonds involving the atoms on the "rim" of the slab also show a contraction, although here a small expansion relative to the bulk, with noticeable larger bond distances, is observed in the innermost part of the structure. A selection of bond distances for the ground state $(TiC)_6$ and $(TiC)_{12}$ clusters and the bulk rock salt structure are compared in Table 1.

It is interesting to compare the differences between these structure and those corresponding to $(MgO)_n$ clusters with the same number of atoms. The ground state structures for small $(MgO)_n$, $n = 6$, 12, clusters tend to exhibit an hexagonal tubular shape [53]. Although the lowest energy

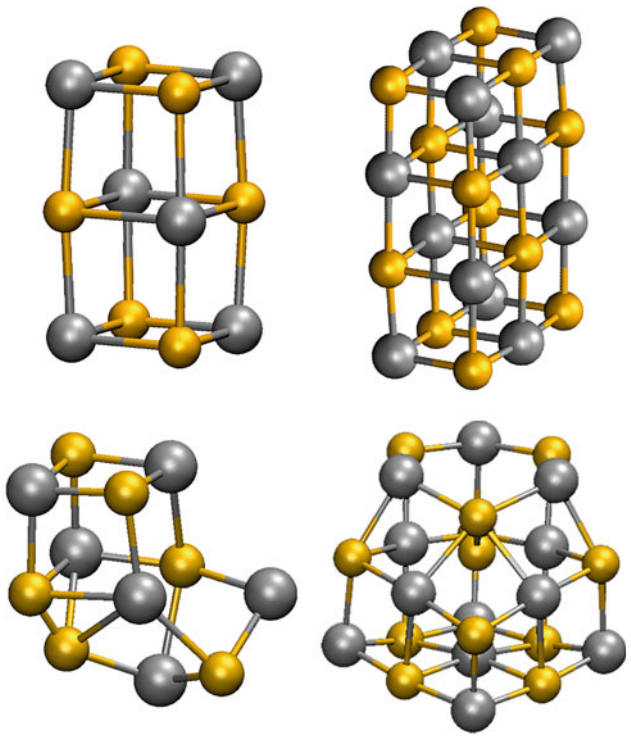

Fig. 1 Lowest energy structures for the $(TiC)_6$ and $(TiC)_{12}$ nanoclusters (*top*), and lowest energy C–C-containing $(TiC)_6$ and $(TiC)_{12}$ nanoclusters (*bottom*) as predicted from global optimization and refined by DFT calculations

Table 1 Smallest and largest TiC distances (Å) found in $(TiC)_6$ and $(TiC)_{12}$ clusters

TiC bonds	$(TiC)_6$	$(TiC)_{12}$
Smallest	1.937	1.899
Largest	2.072	2.195
Bulk calculated	2.161	2.161
Bulk experimental	2.164	2.164

Calculated and experimental TiC distances in the bulk rock salt structure are reported for comparison

structures for $(TiC)_6$ and $(TiC)_{12}$ are bulk-like and thus structurally unlike the corresponding ground states for MgO, most low-energy TiC nanocluster isomers are also found to be low in the energy for MgO. In other words, it is the order of nanocluster isomer stability that is different in each material.

Taking first the comparison between $(TiC)_6$ and $(MgO)_6$ clusters, in addition to the differences in the order of energetic stability, the different $(TiC)_6$ structures are more widely separated in energy (see Fig. 2). Whereas the $(TiC)_6$ isomers are fairly evenly separated throughout a 0.8 eV per TiC unit (eV/TiC) range, the $(MgO)_6$ isomers span a smaller energy interval (<0.6 eV/MgO) and are tightly grouped into two groups: (1) a low-lying pair of isomers

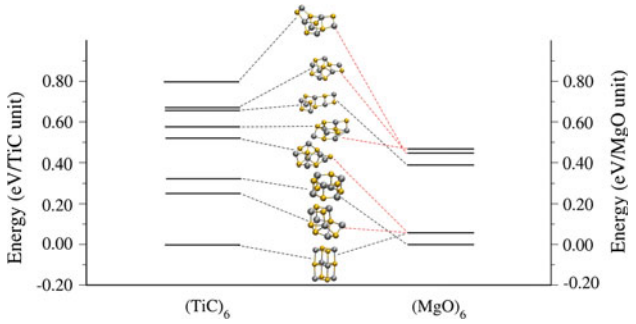

Fig. 2 Relative energies (in eV per TiC or MgO unit) corresponding to the low-energy isomer structures of $(TiC)_6$ and $(MgO)_6$ clusters. The *central part* of the figure shows the calculated structures which are linked to their respective relative energies via *dashed lines*. *Highlighted* by *red dashed lines* are those where structural differences between the two types of clusters are the largest (see Supplementary Information for more detail) (color figure online)

(the hexagonal drum ground state and a bulk cut corresponding to the $(TiC)_6$ ground state) separated by <0.1 eV/MgO and (2) the remaining isomers in a higher lying narrow (<0.2 eV/MgO) energy interval. Of particular note is that some structures obtained for $(TiC)_6$ after full DFT optimization were found to be not stable energy minima for the MgO system. This is the case, for instance, for isomers 2, 4, 5 and 8, where the numbering refers to the order of decreasing stability, in $(TiC)_6$. For $(TiC)_6$, isomers 2 and 5 are especially interesting because both exhibit a C–C bond which is not found to have a correspondence (i.e. a O–O bond) in any low-energy MgO clusters. Attempting to optimize $(TiC)_6$ isomer 2 as a $(MgO)_6$ isomer, for example, converts it to a relatively high-energy isomer with a bulk-like structure. This striking difference between the two materials at the nanoscale is particularly noteworthy as $(TiC)_6$ isomer 2 is only 0.252 eV/TiC higher in energy than the ground state, and it is thus the second most stable cluster found for $(TiC)_6$ (see structure in Fig. 1). Although C–C bonds have not, to our knowledge, been reported previously in stoichiometric TiC clusters, their presence in C-rich non-stoichiometric TiC clusters (e.g. metcars) is well known and is thought to be energetically stabilising [54]. The appearance of the structures with C–C bonds prompted us to study the IR spectra that are reported in Fig. 3 for the bulk ground state cut isomer 1 and for isomer 2. Both calculated IR spectra are quite similar with respect to the position and intensity of their main peaks, except for a low intensity peak observed in the spectra of the C–C bonding isomer that appears at approximately 1,300 cm^{-1} which is due to to the C–C vibrations present in this isomer. Experimentally C-C vibrations in this frequency region have been used to indentify metcars while ruling our bulk-like stoichiometric TiC nanocrystals [55]. The calculated spectra should permit one to differentiate and assign our new stoichiometric, yet C-C-containing, structures from IR measurements. With respect to electronic structure, we also note that the gap between the highest occupied molecular orbital (HOMO) and the lowest unoccupied molecular orbital (LUMO) found for the $(TiC)_6$ ground state is 1.67 eV, while isomer 2 with a C–C bond shows a considerably smaller HOMO–LUMO gap of 0.56 eV.

In the case of $(TiC)_{12}$, one finds trends similar to those already described for the smaller $(TiC)_6$ cluster. Comparing the lowest energy structures obtained for the $(TiC)_{12}$ system with those of $(MgO)_{12}$, we also observe differences in the order of isomer stabilities (see Fig. 4). It is also interesting to remark that the structures for $(TiC)_{12}$ span a significantly larger energy range (0.85 eV/TiC) than in the

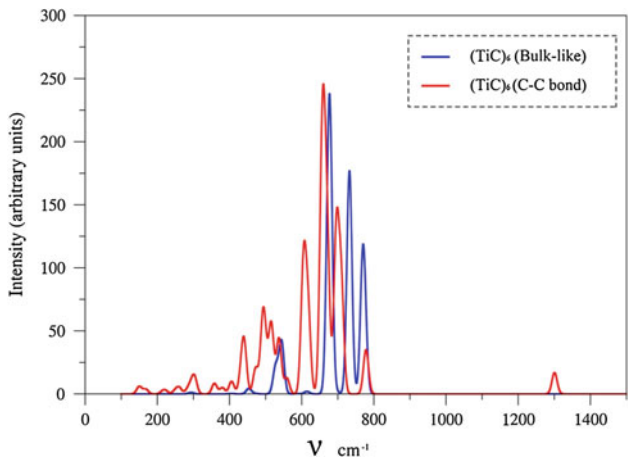

Fig. 3 Calculated IR spectra for two $(TiC)_6$ isomers: the bulk-like ground state isomer (*blue*) and the lowest energy isomer exhibiting C–C bonding (*red*) (color figure online)

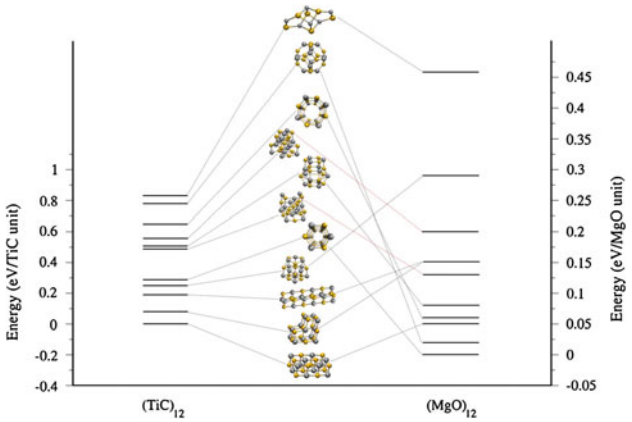

Fig. 4 Relative energies (in eV per TiC or MgO unit) corresponding to the low-energy isomer structures of $(TiC)_{12}$ and $(MgO)_{12}$ clusters. The *central part* of the figure shows the calculated structures which are linked to their respective relative energies via *dashed lines*. *Highlighted* by *red dashed lines* are those where structural differences between the two types of clusters are the largest (see Supplementary Information for more detail) (color figure online)

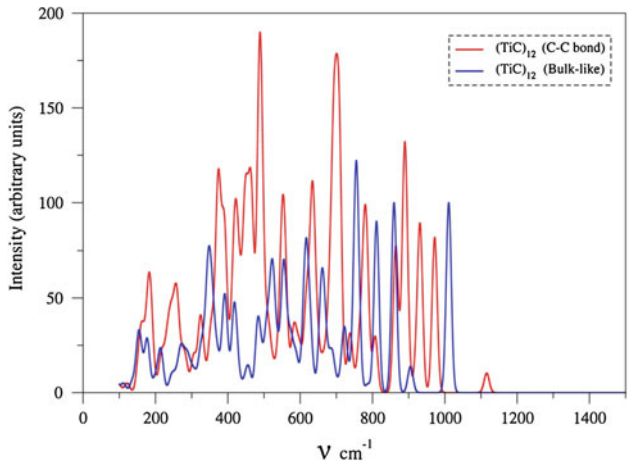

Fig. 5 Calculated IR spectra for two $(TiC)_{12}$ isomers: the bulk-like ground state isomer (*blue*) and the lowest energy isomer exhibiting C–C bonding (*red*) (color figure online)

case of the corresponding $(MgO)_{12}$ cluster (0.47 eV/MgO). Moreover, as for $(TiC)_6$, reasonably stable structures with C–C bonding also appear in the set of low-energy $(TiC)_{12}$ isomers. In particular, $(TiC)_{12}$ isomer 4 contains a C–C bond and is 0.25 eV/TiC higher in energy than the bulk-like-structured $(TiC)_{12}$ ground state (see structure in Fig. 1). Figure 5 presents the calculated IR spectra for the bulk-like ground state $(TiC)_{12}$ isomer and for $(TiC)_{12}$ isomer 4. Here, the spectra are much more complex than for the case of the smaller $(TiC)_6$ clusters. A direct comparison of both spectra is not straightforward, but, as in the case of $(TiC)_6$ cluster, there is a new peak in the spectrum of the isomer with a C–C bond at approximately 1,100 cm^{-1}. As in the previous case, this can be assigned to the C–C vibration. Finally, the $(TiC)_{12}$ HOMO–LUMO gap calculated for the ground state is 1.04 eV, which is smaller than in the case of the $(TiC)_6$ ground state and closer to the bulk, which shows metallic behaviour. The isomer with a C–C bond shows a significantly smaller gap of 0.11 eV, which is in line with the results discussed for $(TiC)_6$.

4 Conclusions

Based on global optimization with interatomic potentials and DFT-based calculations, we confirm that small stoichiometric TiC clusters tend to energetically prefer to exhibit a bulk-like structure. For the $(TiC)_6$ and $(TiC)_{12}$ clusters investigated here, this rock salt-like structure is between 0.1 and 0.3 eV/unit more stable than the next most stable isomers found. This is in clear contrast with some other materials which exhibit the rock salt structure in the bulk such as MgO, for which the lowest energy $(MgO)_6$ and $(MgO)_{12}$ clusters correspond to hexagonal tubular structures. This difference in atomic structure at the nanoscale is likely to be, at least partially, related to the much more covalent character of TiC as compared to MgO, which is a prototypal ionic oxide material. This interpretation is supported by the observation that some of the low-energy isomers of both $(TiC)_6$ and $(TiC)_{12}$ exhibit clear C–C bonding which has no natural low-energy correspondence on MgO clusters. From the calculated IR spectra for the lowest energy isomers of both $(TiC)_6$ and $(TiC)_{12}$, and of the two lowest energy isomers exhibiting C–C bonding, we find distinguishing features which is due to the presence of C–C vibrations. These data may be used to differentiate between these two types of $(TiC)_n$ cluster in experiment.

Acknowledgments Financial support by the Spanish MICINN grant FIS2008-02238, *Generalitat de Catalunya* (grants 2009SGR1041 and XRQTC) is gratefully acknowledged. F. I. acknowledges additional support through the ICREA Academia award for excellence in research.

References

1. Alivisatos AP (1996) Science 271:933–937
2. Daniel MC, Astruc D (2004) Chem Rev 104:293–346
3. Haruta M (1997) Catal Today 36:153–166
4. Kamat PV (2007) J Phys Chem C 111:2834–2860
5. Erwin SC, Zu LJ, Haftel MI, Efros AL, Kennedy TA, Norris DJ (2005) Nature 436:91–94
6. Calais JL (1977) Adv Phys 26:847–885
7. Schwartz K (1987) CRC Crit Rev Solid State Mater Sci 13:211–257
8. Sangthong W, Limtrakul J, Illas F, Bromley ST (2008) J Mater Chem 18:5871–5879
9. Berkdemir C, Castleman AW, Sofo JO (2012) Phys Chem Chem Phys 14:9642–9653
10. Catlow CRA, Bromley ST, Hamad S, Mora-Fonz M, Sokol AA, Woodley SM (2010) Phys Chem Chem Phys 12:786–811
11. Hartke B (2002) Angew Chem Int Ed 41:1468–1487
12. Bromley ST, Moreira I, Neyman KM, Illas F (2009) Chem Soc Rev 38:2657–2670
13. Levy RB, Boudart M (1973) Science 181:547–549
14. Hwu HH, Chen JGG (2005) Chem Rev 105:185–199
15. Viñes F, Rodriguez JA, Liu P, Illas F (2008) J Catal 260:103–112
16. Esposito DV, Chen JG (2011) Energy Environ Sci 4:3900–3912
17. Ren H, Hansgen DA, Kelly TG, Stottlemyer AL, Chen JG (2011) ACS Catal 1:390–398
18. Esposito DV, Hunt ST, Kimmel YC, Chen JG (2012) J Am Chem Soc 134:3025–3033
19. Hsu IJ, Kimmel YC, Willis BG, Chen JG (2012) Chem Comm 48:1063–1065
20. Ono LK, Sudfeld D, Cuenya BR (2006) Surf Sci 600:5041–5050
21. Rodriguez JA, Liu P, Viñes F, Illas F, Takahashi Y, Nakamura K (2008) Angew Chem Int Ed 47:6685–6689
22. Rodriguez JA, Liu P, Takahashi Y, Nakamura K, Viñes F, Illas F (2009) J Am Chem Soc 131:8595–8602
23. Rodriguez JA, Liu P, Takahashi Y, Nakamura K, Viñes F, Illas F (2010) Top Catal 52:393–402

24. Rodriguez JA, Feria L, Jirsak T, Takahashi Y, Nakamura K, Illas F (2010) J Am Chem Soc 132:3177–3186
25. Florez E, Gomez T, Liu P, Rodriguez JA, Illas F (2010) ChemCatChem 2:1219–1222
26. Florez E, Gomez T, Rodriguez JA, Illas F (2011) Phys Chem Chem Phys 13:6865–6871
27. Vidal AB, Feria L, Evans J, Takahashi Y, Liu P, Nakamura K, Illas F, Rodriguez JA (2012) J Phys Chem Lett 3:2275–2280
28. Guo BC, Wei S, Purnell J, Buzza SA, Castleman AW (1992) Science 256:515–516
29. Pillgrim JS, Duncan MA (1993) J Am Chem Soc 115:6858–6961
30. Wei S, Guo BC, Deng HT, Kerns K, Purnell J, Buzza SA, Castleman AW (1994) J Am Chem Soc 116:4475–4476
31. Duncan MA (1997) J Clust Sci 8:239–266
32. Rohmer MM, Bérnard M, Poblet JM (2000) Chem Rev 100:495–542
33. Patzschke M, Sundholm D (2005) J Phys Chem B 109:12503–12508
34. Li S, Wu H, Wang LS (1997) J Am Chem Soc 119:7417
35. Reddy BV, Khanna SN (1994) J Phys Chem 98:9946–9949
36. von Helden G, Tielens AGGM, van Heijnsbergen D, Duncan MA, Hony S, Waters LBFM, Meijer G (2000) Science 288:313–316
37. Wales DJ, Doye JPK (1997) J Phys Chem A 101:5111–5116
38. Carrasco J, Illas F, Bromley ST (2007) Phys Rev Lett 99:235502
39. Roberts C, Johnston RL (2001) Phys Chem Chem Phys 3:5024–5034
40. Erkoc S (1989) Phys Stat Sol (b) 152:447–454
41. Gale JD, Rohl AL (2003) Mol Simul 29:291–341
42. Kresse G, Hafner J (1993) Phys Rev B 47:558–561
43. Kresse G, Hafner J (1994) Phys Rev B 49:14251–14269
44. Kresse G, Furthmüller J (1996) Phys Rev B 54:11169–11186
45. Kresse G, Furthmüller J (1996) J Comp Mat Sci 6:15–50
46. Blöchl PE (1994) Phys Rev B 50:17953–17979
47. Kresse G, Joubert D (1999) Phys Rev B 59:1758–1775
48. Perdew JP, Wang Y (1992) Phys Rev B 45:13244–13249
49. Perdew JP, Wang Y (1993) Phys Rev B 48:4978
50. Valcárcel A, Ricart JM, Illas F, Clotet A (2004) J Phys Chem B 108:18297–18305
51. Happel M, Luckas N, Viñes F, Sobota M, Laurin M, Görling A, Libuda J (2011) J Phys Chem C 115:479–491
52. Lukas N, Viñes F, Happel M, Desikusumastuti A, Libuda J, Görling A (2010) J Phys Chem C 114:13813–13824
53. Bawa F, Panas I (2002) Phys Chem Chem Phys 4:103–108
54. Joswig J-O, Springborg M (2008) J Chem Phys 129:134311
55. van Heijnsbergen D, von Helden G, Duncan MA, van Roij AJA, Meijer G (1999) Phys Rev Lett 83:4983